Computer Assisted Mechanics and Engineering Sciences, **12**: 329–339, 2005.

On the numerical prediction of the anisotropic elastic properties in thin-walled structures made from short-fiber reinforced plastics[1]

Holm Altenbach, Konstantin Naumenko
Martin-Luther-Universität Halle-Wittenberg, Fachbereich Ingenieurwissenschaften, Lehrstuhl für Technische Mechanik, Halle(Saale), Germany

Sergiy Pylypenko
Otto-von-Guericke Universität, Graduiertenkolleg "Mikro-Makro-Wechselwirkungen in strukturierten Medien und Partikelsystemen", Magdeburg, Germany

(Received February 26, 2004)

The paper presents a model which allows to estimate the elastic properties of thin-walled structures manufactured by means of injection molding. The starting point is the numerical prediction of the microstructure of a short fiber reinforced composite induced during the filling stage of the manufacturing process. For this purpose the commercial program Moldflow Plastic Insight® (MPI) is used. The result of the filling simulation characterizing the fiber microstructure is a second rank orientation tensor. The elastic material properties after the processing are locally dependent on the orientational distribution of the fibers. The constitutive model is formulated by means of the orientational averaging for the given orientation tensor. The tensor of elastic material properties is computed and translated into the format suitable for the stress-strain analysis based on the ANSYS® finite element code. The influence of technological manufacture parameters on the microstructure and the elastic properties is discussed with the help of two examples a center-gated disk and a shell of revolution.

1. Introduction

The use of short-fiber reinforced thermoplastics (fiber length around 0.1–1 mm, fiber diameter around 0.01 mm, fiber volume fraction 15–40%) has been rapidly increasing during the last years in many industrial branches, e.g. automobile industry, pump industry, etc. [13, 17, 20, 22]. Various load bearing components (usually thin-walled structures) are manufactured from these materials by injection molding. This manufacturing process is of particular interest because of highly automated production, relatively short cycle time and low production costs. Furthermore, the principal advantage of this process over other methods of manufacturing is the possibility of mass production of articles with a desired geometrical complexity. However, the mechanical properties of particle reinforced materials are quite poor if compared with those of materials reinforced by continuous fibers. In addition, the stiffness and the strength of short-fiber reinforced composites and thin-walled structures manufactured from these materials are highly dependent on the orientation and the distribution of particles. As show many experimental observations, the fiber orientation induced by injection molding has significant spatial variations within the part, e.g. [7, 19, 22, 23]. The orientation of the fibers and their distribution density depend on various factors (fiber length, volume fraction, fiber concentration and among other), process conditions and the geometry of the mold

[1]Extended version of the first part of the lecture held during the IX International Conference Numerical Methods in Continuum Mechanics (Žilina, Slovakia, 9–12 September 2003).

cavity, e.g. [14, 23]. Therefore, the key step in the preliminary design of load bearing components lies in the prediction of the fiber orientation pattern for given manufacturing conditions.

2. Theoretical background

2.1. Modelling of the flow induced fiber microstructure

For the numerical predictions of the fiber orientation we have used the MPI code. Let us briefly outline the approach realized in the MPI code for the description of the fiber orientation during the flow of suspensions. A detailed discussion is presented in the reviews [11, 12, 21]. The suspension is modelled as a quasi-homogeneous anisotropic medium. According to this approach, the main problem consists in the formulation of a rheological equation allowing us to relate the stresses caused by the liquid flow with local characteristics of the motion. For a slow motion of a viscous liquid such an equation is [6]

$$\boldsymbol{\sigma} = -p\mathbf{E} + \boldsymbol{\mu}\cdot\cdot\boldsymbol{\Lambda}, \qquad \boldsymbol{\Lambda} = \nabla\mathbf{V}, \tag{1}$$

where $\boldsymbol{\sigma}$ is the stress tensor, p is the pressure in the medium, $\mathbf{E}$ is the second-rank unit tensor, $\mathbf{V}$ is the velocity of the medium, $\boldsymbol{\mu}$ is the fourth-rank viscosity tensor, which is determined by the local state of the medium. Different approaches for determining the quantity $\boldsymbol{\mu}$ are discussed in the review on suspension rheology [18] and in the monograph [15]. The most popular approach is based on the method of orientational averaging. As an example, we will consider the model offered in [9] for describing semiconcentrated suspensions:

$$\boldsymbol{\sigma} = -p\mathbf{E} + \mu(\boldsymbol{\Lambda} + \boldsymbol{\Lambda}^{\mathrm{T}})\cdot\cdot\left[{}^{(4)}\mathbf{E} + \frac{nl^2}{12\mu}\zeta_p\,{}^{(4)}\mathbf{A}\right]. \tag{2}$$

Here n is the number of particles in a unit volume, l is the length of fibers, μ is the polymer viscosity, and ζ_p is a coefficient determined by the formula

$$\zeta_p = \frac{2\pi\mu l}{\ln(2h/d)},$$

where d is the fiber diameter; $h = (nl)^{-1/2}$ for oriented fibers and $h = (nl^2)^{-1}$ for a random orientation. In Eq. (2) ${}^{(4)}\mathbf{E}$ is the fourth-rank unit tensor and ${}^{(4)}\mathbf{A}$ is a fourth-rank tensor representing the current state of fiber orientation,

$${}^{(4)}\mathbf{A} = \int_{(S)} \Psi(\mathbf{m})\mathbf{m}\otimes\mathbf{m}\otimes\mathbf{m}\otimes\mathbf{m}\,\mathrm{d}S, \tag{3}$$

where $\Psi(\mathbf{m})$ is the distribution density of fiber orientation, $\mathbf{m}$ is a unit vector along the particle axis, $\mathrm{d}S$ is a differential element on the unit sphere. Model (2) is most popular in numerical calculations of injection molding proceses (see, for example, [2, 8]).

For the orientation density Ψ we write [10, 21]

$$\dot{\Psi} + \nabla_s\cdot(\Psi\boldsymbol{\omega} - d_r\nabla_s\Psi) = 0, \tag{4}$$

where $\dot{(\ldots)}$ is the material derivative and ∇_s is the tangential differential operator on the unit sphere

$$\nabla_s(\ldots) = \mathbf{e}_k\epsilon_{ijk}m_i\frac{\partial(\ldots)}{\partial m_j}, \qquad \mathbf{m}\cdot\mathbf{m} = 1,$$

where ϵ_{ijk} is the Levi–Civita symbol. In Eq. (4) $\boldsymbol{\omega}$ the angular velocity of a particle and d_r is the empirical coefficient of rotational diffusion, which was offered in [1] for describing the interaction

between the particles. According to [1] for the quantity $\boldsymbol{\omega}$ we assumed the solution obtained by Jeffery [16] for the angular velocity of an ellipsoidal particle in an infinite field of viscous liquid. For an ellipsoid of revolution this solution takes the form [4]

$$\boldsymbol{\omega} = (\boldsymbol{\phi} + \lambda \mathbf{m} \times \mathbf{D} \cdot \mathbf{m}), \qquad \lambda = \frac{a^2 - b^2}{a^2 + b^2}, \tag{5}$$

where a and b are the semiaxes of the ellipsoid, $\mathbf{D}$ is the strain rate tensor and $\boldsymbol{\phi}$ is the spin vector of the undisturbed flow, which can be obtained from the velocities:

$$\mathbf{D} = \frac{1}{2}(\boldsymbol{\Lambda} + \boldsymbol{\Lambda}^{\mathrm{T}}), \qquad \mathrm{tr}(\mathbf{D}) = 0, \qquad \boldsymbol{\phi} = \frac{1}{2}\nabla \times \mathbf{V} = \frac{1}{2}\boldsymbol{\Lambda}_{\times}.$$

If we introduce moments of the distribution function $\Psi(\mathbf{m})$,

$$^{(n)}\mathbf{A} = \int_{(S)} \Psi(\mathbf{m}) \mathbf{m}^{\otimes n} \mathrm{d}S, \qquad n = 2, 4, \ldots,$$

where $^{(n)}\mathbf{A}$ is an n-th-rank orientation tensor and $(\ldots)^{\otimes n}$ is the n-th tensor product, Eq. (4) with regard to the angular velocity (5) is transformed into an infinite system of coupled equations. The first two of them are

$$\begin{aligned}
^{(2)}\dot{\mathbf{A}} &= {}^{(2)}\mathbf{A}\cdot\mathbf{W} - \mathbf{W}\cdot{}^{(2)}\mathbf{A} + \lambda(\mathbf{D}\cdot{}^{(2)}\mathbf{A} + {}^{(2)}\mathbf{A}\cdot\mathbf{D} - 2{}^{(4)}\mathbf{A}\cdot\cdot\mathbf{D}) - 6d_r\left({}^{(2)}\mathbf{A} - \frac{1}{3}\mathbf{E}\right), \\
^{(4)}\dot{\mathbf{A}} &= {}^{(4)}\mathbf{A}\cdot\mathbf{W} - \mathbf{W}\cdot{}^{(4)}\mathbf{A} + \lambda(\mathbf{D}\cdot{}^{(4)}\mathbf{A} + {}^{(4)}\mathbf{A}\cdot\mathbf{D} - 4{}^{(6)}\mathbf{A}\cdot\cdot\mathbf{D}) \\
&\quad - \mathbf{e}_i \otimes \mathbf{W}\cdot{}^{(4)}\mathbf{A}\cdot\mathbf{e}_i + \mathbf{e}_i\cdot{}^{(4)}\mathbf{A}\cdot\mathbf{W}\otimes\mathbf{e}_i + \lambda\left(\mathbf{e}_i\otimes\mathbf{D}\cdot{}^{(4)}\mathbf{A}\cdot\mathbf{e}_i + \mathbf{e}_i\cdot{}^{(4)}\mathbf{A}\cdot\mathbf{D}\otimes\mathbf{e}_i\right) \\
&\quad + 2d_r\Big(\mathbf{E}\otimes{}^{(2)}\mathbf{A} + {}^{(2)}\mathbf{A}\otimes\mathbf{E} + {}^{(2)}\mathbf{A}\cdot\mathbf{e}_k\otimes\mathbf{E}\otimes\mathbf{e}_k + \mathbf{e}_k\otimes{}^{(2)}\mathbf{A}\otimes\mathbf{e}_k \\
&\quad + {}^{(2)}\mathbf{A}\cdot\mathbf{e}_i\otimes\mathbf{e}_k\otimes\mathbf{e}_i\otimes\mathbf{e}_k + \mathbf{e}_i\otimes\mathbf{e}_k\otimes\mathbf{e}_i\otimes\mathbf{e}_k\cdot{}^{(2)}\mathbf{A} - 10{}^{(4)}\mathbf{A}\Big).
\end{aligned} \tag{6}$$

Here, $\mathbf{W} = \boldsymbol{\phi} \times \mathbf{E}$ is the flow vorticity tensor, $\mathbf{e}_i$ is an arbitrary orthonormal basis, and the summation is carried out over the subscripts repeated twice. In [1] Eqs. (6) are given in the index notation. In practical calculations, $^{(2)}\mathbf{A}$ is usually found from the first evolutionary equation and $^{(4)}\mathbf{A}$ from the closure approximation. In the present study the hybrid closure approximation [1] incorporated in the MPI code is used:

$$\begin{aligned}
^{(4)}\mathbf{A} &\approx (1-f)\,{}^{(4)}\mathbf{A}^L + f\,{}^{(4)}\mathbf{A}^Q, \qquad f = 1 - 27\det\left({}^{(2)}\mathbf{A}\right), \qquad {}^{(4)}\mathbf{A}^Q = {}^{(2)}\mathbf{A}\otimes{}^{(2)}\mathbf{A}, \\
^{(4)}\mathbf{A}^L &= \frac{1}{7}\Big(\mathbf{E}\otimes{}^{(2)}\mathbf{A} + {}^{(2)}\mathbf{A}\otimes\mathbf{E} + {}^{(2)}\mathbf{A}\cdot\mathbf{e}_k\otimes\mathbf{E}\otimes\mathbf{e}_k + \mathbf{e}_k\otimes{}^{(2)}\mathbf{A}\otimes\mathbf{e}_k \\
&\quad + {}^{(2)}\mathbf{A}\cdot\mathbf{e}_i\otimes\mathbf{e}_k\otimes\mathbf{e}_i\otimes\mathbf{e}_k + \mathbf{e}_i\otimes\mathbf{e}_k\otimes\mathbf{e}_i\otimes\mathbf{e}_k\cdot{}^{(2)}\mathbf{A}\Big) \\
&\quad + \frac{1}{35}(\mathbf{E}\otimes\mathbf{E} + \mathbf{e}_k\otimes\mathbf{E}\otimes\mathbf{e}_k + \mathbf{e}_i\otimes\mathbf{e}_k\otimes\mathbf{e}_i\otimes\mathbf{e}_k).
\end{aligned} \tag{7}$$

Thus, the polymeric suspension is modeled as a viscous incompressible anisotropic medium with the constitutive equation (2) and the evolution equation (6) based on the closure approximation (7). In the process of numerical solution by the finite element method, the evolution equation (6) is additionally integrated with respect to time and to Eq. (7). As a result, we obtain a second-rank orientation tensor $^{(2)}\mathbf{A}$, which is calculated at the nodes of a finite element mesh and is responsible for the final distribution of the fibers.

2.2. Governing equations for the filling phase

Let us assume that the fluid occupies a bounded domain Ω with the boundary Γ. The governing equations describing the flow of the suspension must include

- the balance of momentum, e.g. [5],

$$\rho \frac{D}{Dt}\mathbf{V} = \rho \mathbf{f} + \nabla \cdot \boldsymbol{\sigma}, \tag{8}$$

where $\mathbf{f}$ is the vector of body forces,

- the balance of mass, e.g. [5],

$$\rho = \text{const} \quad \Longrightarrow \quad \nabla \cdot \mathbf{V} = 0, \tag{9}$$

- the energy balance

$$\rho c_p \frac{DT}{Dt} = \boldsymbol{\sigma} \cdot\cdot \nabla \mathbf{V} + \nabla \cdot (k \nabla T), \tag{10}$$

where T is the temperature, c_p is the coefficient of heat capacity under constant pressure, k is the coefficient of heat conductivity,

- the constitutive equation, for example Eq. (2),
- the evolution equation for the structure tensors, for example first Eq. of (6),
- the closure approximation, for example Eq. (7),
- the boundary conditions on Γ

$$\mathbf{V} = \bar{\mathbf{V}}, \qquad T = \bar{T}, \qquad \mathbf{x} \in \Gamma, \qquad p = 0, \qquad \mathbf{x} \in \Gamma_f,$$

where Γ_f is the boundary of the free surface,

- the initial conditions on a given part of the domain

$$\mathbf{V}(\mathbf{x}, 0) = \mathbf{V}^0, \qquad {}^{(2)}\mathbf{A}(\mathbf{x}, 0) = {}^{(2)}\mathbf{A}^0.$$

The numerical solution of the presented equations in the general case of the complex cavity geometry requires a great effort. The discussions related to the numerical solutions and possible simplifications of the equations can be found in reviews [11, 21]. The commonly used simplification is the Hele–Shaw approximation, which is applicable to the analysis of the flow in narrow gaps, [2, 11, 21]. The Hele–Shaw approximation is also the basis of commercial codes for the injection molding simulations.

2.3. Estimation of the elastic stiffness properties

The output from the MPI is the second rank orientation tensor ${}^{(2)}\mathbf{A}$. In order to perform the structure analysis it is necessary to compute the elastic stiffness tensor. This can be made in two steps. The first step is the model for the transversely isotropic unidirectional elastic composite

$$\tilde{\boldsymbol{\sigma}}(\mathbf{m}) = \lambda \mathrm{tr}\boldsymbol{\epsilon}\, \mathbf{E} + \alpha \boldsymbol{\epsilon} \cdot\cdot \mathbf{N}\, \mathbf{E} + 2\mu_T \boldsymbol{\epsilon} + \alpha \mathrm{tr}\boldsymbol{\epsilon}\, \mathbf{N} + \beta \boldsymbol{\epsilon} \cdot\cdot \mathbf{N} \otimes \mathbf{N} + 2(\mu_L - \mu_T)[\mathbf{N} \cdot \boldsymbol{\epsilon} + \boldsymbol{\epsilon} \cdot \mathbf{N}], \tag{11}$$

$$\mathbf{N} = \mathbf{m} \otimes \mathbf{m}.$$

In Eq. (11) $\tilde{\boldsymbol{\sigma}}(\mathbf{m})$ is the stress tensor, $\boldsymbol{\epsilon}$ is the strain tensor, α, β, λ, μ_L and μ_T are five invariants which must be determined from the engineering constants. The engineering constants are usually available in the MPI material database.

The second step is the averaging of Eq. (11) over all directions of the vector $\mathbf{m}$. Using the function $\Psi(\mathbf{m})$ of fiber orientation distribution we obtain

$$\begin{aligned}\boldsymbol{\sigma} = \int_{(S)} \Psi(\mathbf{m})\,\tilde{\boldsymbol{\sigma}}(\mathbf{m})\,\mathrm{d}S \;&=\; \mathrm{tr}\boldsymbol{\epsilon}\,\mathbf{E}\left[\alpha_* + \frac{2}{3}\beta_* + \frac{1}{9}\eta_*\right] + \boldsymbol{\epsilon}\left[2\gamma_* + \frac{4}{3}\xi_*\right] \\ &+\; \left(\beta_* + \frac{1}{9}\eta_*\right)\boldsymbol{\epsilon}\cdot\cdot(\mathbf{B}\otimes\mathbf{E} + \mathbf{E}\otimes\mathbf{B}) \\ &+\; 2\xi_*(\mathbf{B}\cdot\boldsymbol{\epsilon} + \boldsymbol{\epsilon}\cdot\mathbf{B}) + \eta_*\boldsymbol{\epsilon}\cdot\cdot\mathbf{B}\otimes\mathbf{B},\end{aligned} \tag{12}$$

where

$$\alpha_* = \lambda + \beta\frac{1-f}{35}, \quad \beta_* = \alpha + \beta\frac{1-f}{7}, \quad \gamma_* = \mu_T + \beta\frac{1-f}{35}, \quad \xi_* = \mu_L - \mu_T + \beta\frac{1-f}{7}, \quad \eta_* = f\beta.$$

Here we have used the hybrid closure approximation for the forth rank tensor ${}^{(4)}\mathbf{A}$, incorporated in the MPI. From Eq. (12) we observe that the elasticity law consist of two parts. The first part is the usual isotropic part. The second part is the anisotropic one which depends on the deviatoric part of the tensor ${}^{(2)}\mathbf{A}$, which can be expressed as $\mathbf{B} = {}^{(2)}\mathbf{A} - \frac{1}{3}\mathbf{E}$. For the statistically isotropic (uniform) orientation distribution we find that $\mathbf{B} = \mathbf{0}$ and the second part in Eq. (12) vanishes.

Based on Eq. (12) the stiffness constants can be computed and transformed into the form necessary for the ANSYS-based finite element analysis. The subroutine allowing to translate the output from the fill simulation into the ANSYS-command file for the structure analysis has been developed and tested.

3. Numerical investigation of the sensitivity of the composite microstructure

The stiffness of load bearing components made from thermoplastics reinforced by short fibers depends on the orientation of the fibres. Hence, changing orientation of fibres probably allows the creation of products with identical geometry and various stiffness.

To make an analysis of the sensitivity of the composite microstructure for complex geometry and to allocate tendencies of influence of technological parameters of manufacturing on the orientation of fibres is difficult. Therefore it is necessary to take the advantage of simple geometry and to allocate factors influencing the orientation of fibres. As such geometry the center-gated disk is taken. For the disk the following geometrical parameters were used: radius $R = 76.2$ mm, thickness $h = 3.18$ mm (see Fig. 1).

It is necessary to determine parameters which can affect the orientation of fibres. Key parameters during manufacturing of such composite materials are:

- temperature of the melt T_{inlet},
- temperature of the cavity wall T_{wall},
- time of filling t_{fill}.

There are also other factors influencing the orientation of fibres, for example, the use of various materials, and the variation of the arrangement and type of the gate. The variation of these

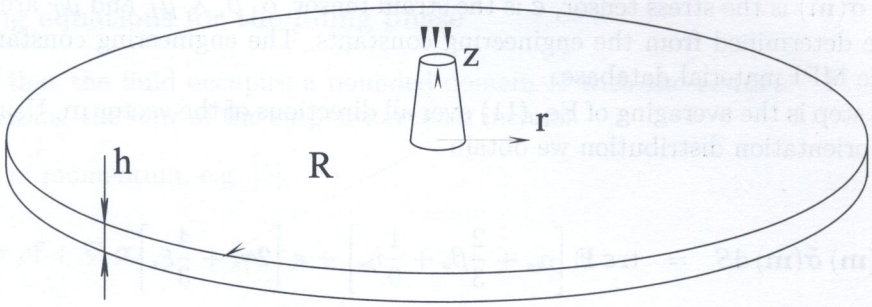

Fig. 1. Model of a center-gated disk

parameters undoubtedly makes essential change the microstructure of the composite material. However, such ways of influence are expensive and their constructive realization is not always possible, therefore they are used seldom.

We made a series of calculations based on MPI code at various temperatures of melt and cavity, and also time of filling. As a material is taken: Du Pont Zytel® 70G43L with 43% of glass fibres. For calculation of the given model the finite element grid containing 1632 elements has been used.

As it is marked above, orientation of fibres is determined by the second rank tensor. We shall consider distribution of the first principal value of the orientation tensor over the thickness of the disk vs. of technological regimes. Two points located on the radial distance from the center of disk are taken: $R_1 = 36$ mm, $R_2 = 64$ mm.

In the first stage of work we calculate orientation tensor at various temperatures of melt. Parameters of calculations are:

- $T_{\text{inlet}} = 267, 277, 287, 305°\text{C}$,
- $T_{\text{wall}} = 74°\text{C}$,
- $t_{\text{fill}} = 2.5$ s.

Results of calculations of the first principal value of the orientation tensor over the thickness of the disk are presented in Fig. 2.

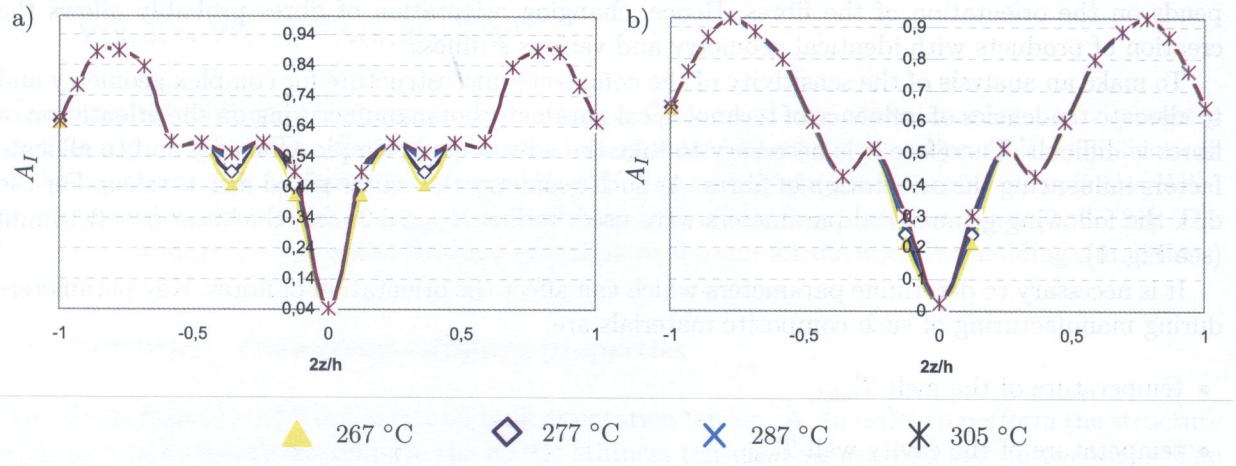

Fig. 2. Variation of temperature of melt, a) control point R_1, b) control point R_2

In the second stage we performed calculations at various temperatures of the wall of the cavity. Parameters of calculations were:

- $T_{\text{inlet}} = 277°\text{C}$,
- $T_{\text{wall}} = 64, 74, 84, 120°\text{C}$,
- $t_{\text{fill}} = 2.5$ s.

The results of calculations are presented in Fig. 3.

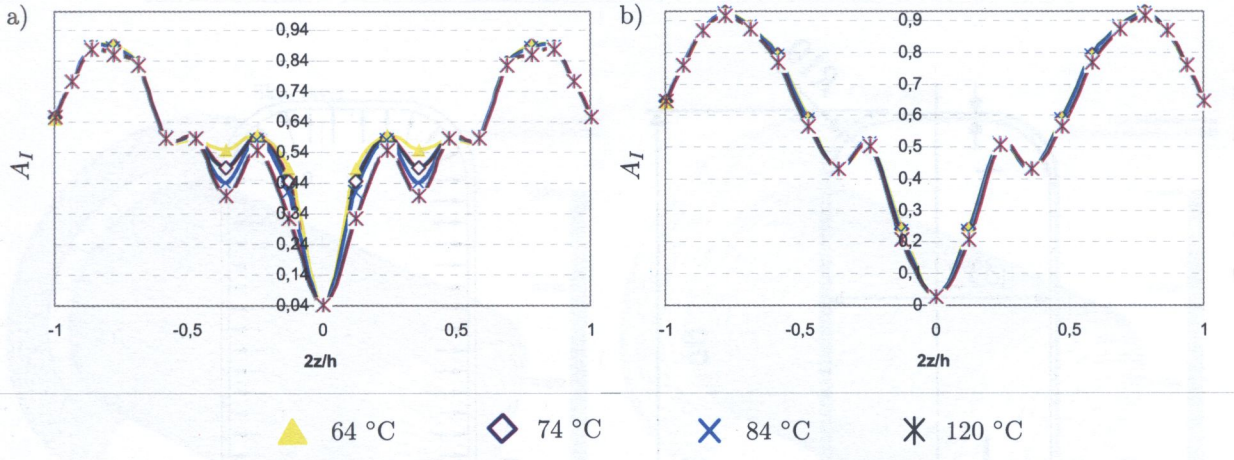

Fig. 3. Variation of temperature of cavity wall, a) control point R_1, b) control point R_2

On the third stage we made calculations at various time of filling. We used the following parameters of calculations:

- $T_{\text{inlet}} = 277°\text{C}$,
- $T_{\text{wall}} = 74°\text{C}$,
- $t_{\text{fill}} = 0.5, 2, 3, 5$ s.

The results of calculations are presented in Fig. 4.

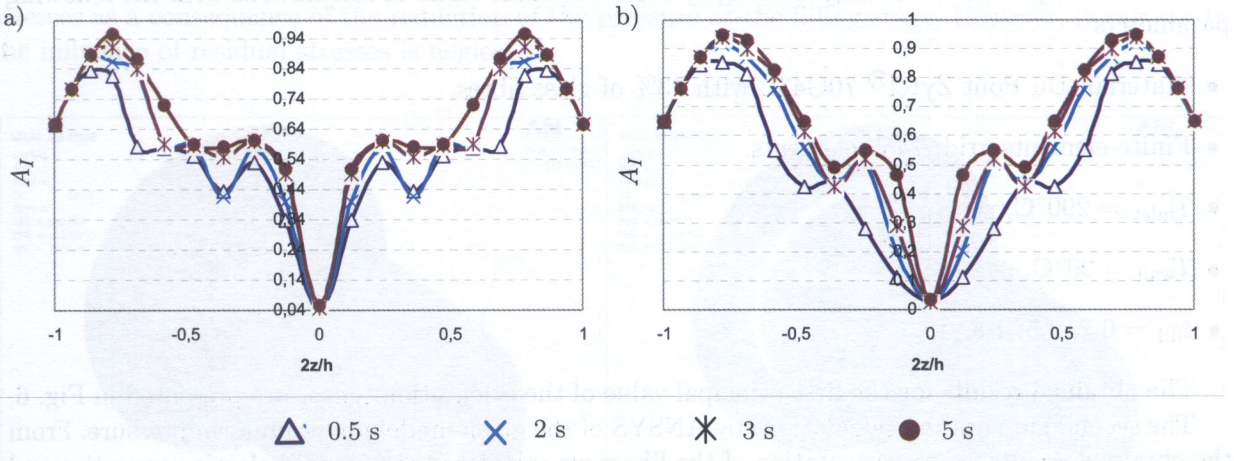

Fig. 4. Variation of time of filling, a) control point R_1, b) control point R_2

From the calculations it is clearly seen that only the time of filling has a significant influence on the elastic properties since the microstructure is affected by this parameter. The other parameters practically do not influence the composite microstructure and must be chosen according to recommendations of the manufacturer of the composite material.

4. Sensitivity of elastic properties of a thin-walled shell

The numerical analysis of the sensitivity of the microstructure of a composite to technological parameters for a simple geometry has shown that only the filling time (i.e. the speed of the flow) influences the orientation of the fibres. Now we will show how the stress-strain state is affected by the change of orientation of the fibers. The geometry of the structure under consideration the loading case and the assumed boundary conditions are presented on Fig. 5a.

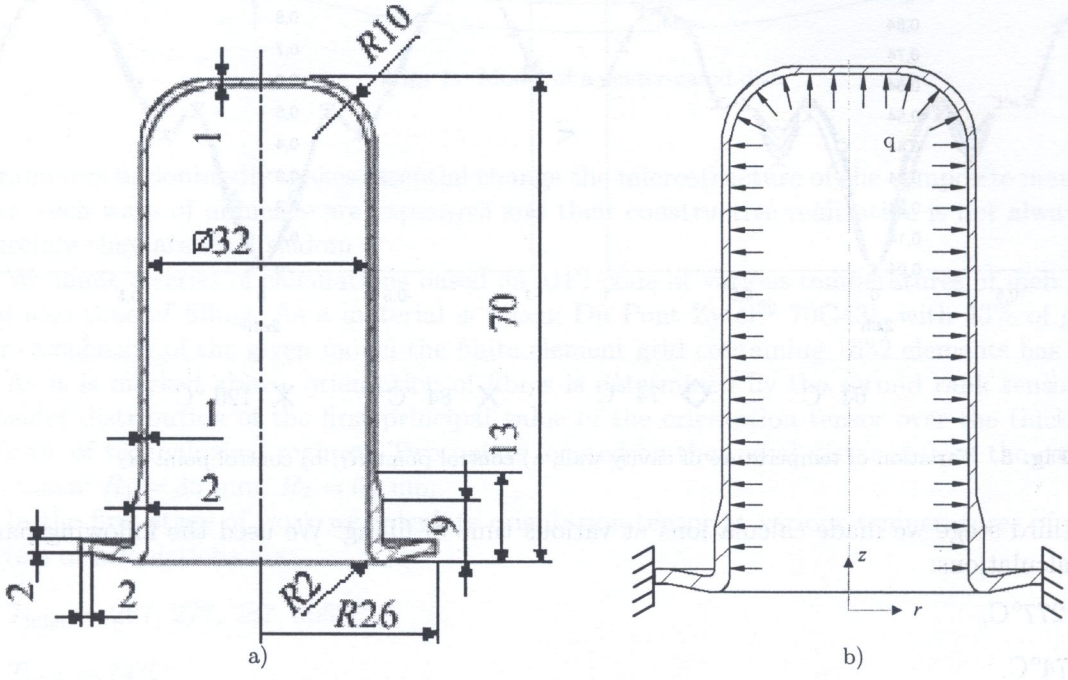

Fig. 5. Model of shell of revolution, a) geometry, b) mechanical model

The first step is the modelling of filling by MPI. We made series of calculations with the following parameters:

- Material: Du Pont Zytel® 70G43L with 43% of glass fibres,
- Finite-elements grid: 7458 elements,
- $T_{\text{inlet}} = 290°\text{C}$,
- $T_{\text{wall}} = 90°\text{C}$,
- $t_{\text{fill}} = 0.2, 0.5, 1$ s.

The obtained results for the first principal value of the orientation tensor are presented in Fig. 6.

The second step are the calculations by ANSYS of the given model under uniform pressure. From the obtained results for the orientation of the fibers we calculate the averaged elastic properties and transmit them into ANSYS. The mechanical model for the ANSYS calculations is shown in Fig. 5b. The loading is the uniform pressure $q = 8$ MPa, the boundary conditions correspond to the clamped flange.

The distributions of the stress components for the three cases of the filling time do not change, therefore on Fig. 7 we present only the distributions for the case $t_{\text{fill}} = 0.2$ s.

The numerical results, for the maximal stresses and displacement are presented in Table 1.

Table 1. Results for the maximal values of the axial displacement and the stresses for various of the times of filling

Time of filling, s	$w_{\max}$, mm	$\sigma_{r_{\max}}$, MPa	$\sigma_{\theta_{\max}}$, MPa	$\sigma_{z_{\max}}$, MPa
0.2	2.747	521	395	266
0.5	2.776	507	319	260
1.0	2.785	488	318	269

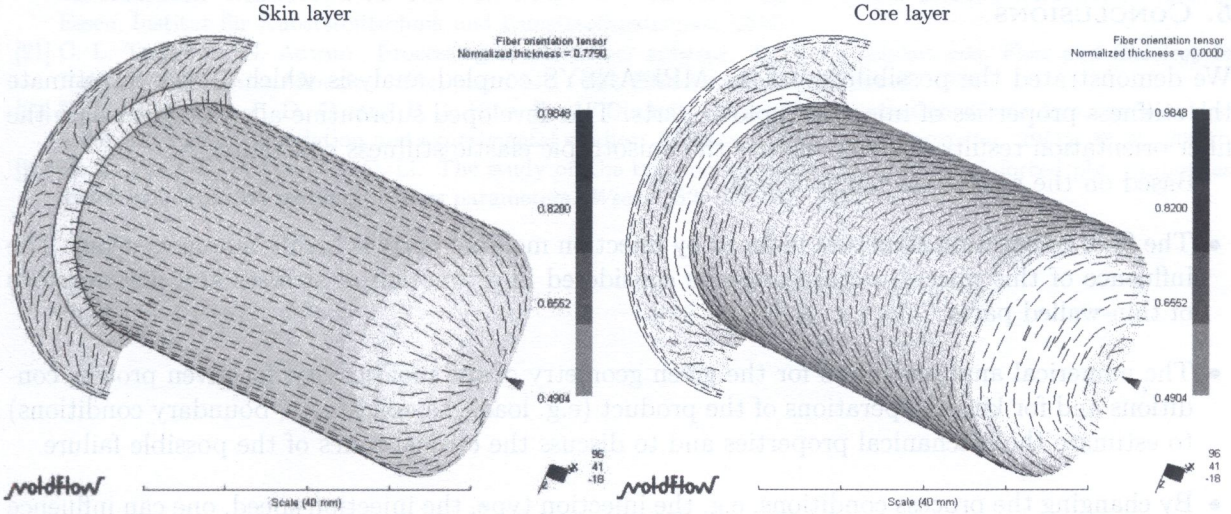

Fig. 6. First principal value of the orientation tensor $^{(2)}\mathbf{A}$

The obtained results illustrate that the changes of the microstructure of a composite in dependence of the variation of the time of filling influence the stress-strain state. The change of filling time from 0.2 till 1 s. has led to decrease the radial stress (6 %) and the circumferential stress (19 %). In additional we can assume that, the decrease of the filling time may lead to the decrease of residual stresses as a consequence of the reduction of the pressure at the filling stage. However, in our study the influence of residual stresses is neglected.

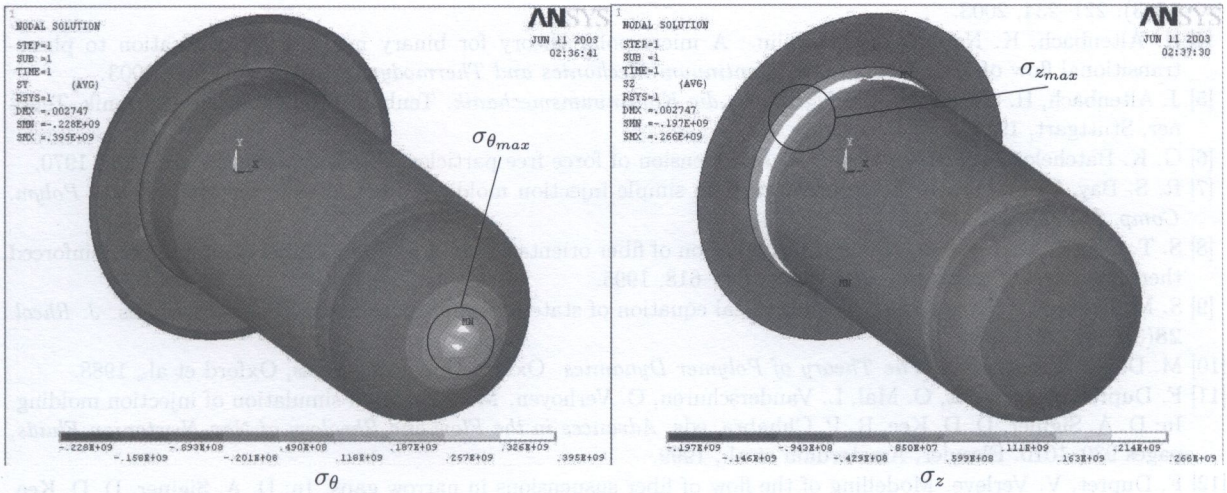

Fig. 7. Distributions of circumferential and axial stresses ($t_{\text{fill}} = 0.2$ s.)

Let us note that there are various possibilities to affect the orientation of fibres. Those are the use of other material or the change of the arrangement and the type of the injection gate [3]. Both possibilities are expensive. The use of the last way is not possible since the process of development and manufacturing of a new cavity is very expensive, besides is not always possible. For example, cavities for parts similar to considered, must have a gate on an axis of rotation, for prevention of defects during manufacturing (air traps, weld line, etc.). For the given part such a point is only one and therefore the change of the gate positions is not possible.

5. Conclusions

We demonstrated the possibilities of the MPI–ANSYS coupled analysis which allows to estimate the stiffness properties of injection molded parts. The developed subroutine allows to translate the fiber orientation results and to compute the anisotropic elastic stiffness constants.

Based on the results we can conclude:

- The fiber orientation structure induced by injection molding parts is highly inhomogeneous. The influence of this microstructure must be considered in estimation of stresses and deformations of thin-walled parts.
- The numerical analysis allows for the given geometry of the mold cavity, for given process conditions and for known operations of the product (e.g. loads, temperatures, boundary conditions) to estimate the mechanical properties and to discuss the critical zones of the possible failure.
- By changing the process conditions, e.g. the injection type, the injection speed, one can influence the fiber orientation microstructure. This can improve the elastic stiffness and strength properties in zones with critical stress states.

References

[1] S. G. Advani, C. L. Tucker. The use of tensors to describe and predict fiber orientation in short fibers composites. *J. Rheol.* **31**(48): 751–784, 1987.

[2] M. C. Altan, S. Subbiah, S. I. Güçeri, R. B. Pipes. Numerical prediction of three-dimensional fiber orientation in hele-shaw flows. *Polym. Eng. Sci.* **30**(14): 848–859, 1990.

[3] H. Altenbach, K. Naumenko, G. I. Lvov, S. N. Pylypenko. Numerical estimation of the elastic properties of thin-walled structures manufactured from short-fiber-reinforced thermoplastics. *Mechanics of Composite Materials* **39**(3): 221–234, 2003.

[4] H. Altenbach, K. Naumenko, P. Zhilin. A micro-polar theory for binary media with application to phase-transitional flow of fiber suspensions. *Continuum Mechanics and Thermodynamics* **15**: 539–570, 2003.

[5] J. Altenbach, H. Altenbach. *Einführung in die Kontinuumsmechanik*. Teubner Studienbücher Mechanik. Teubner, Stuttgart, 1994.

[6] G. K. Batchelor. The stress system in a suspension of force free particles. *J. Fluid Mech.* **41**: 545–570, 1970.

[7] R. S. Bay, C. L. Tucker. Fiber orientation in simple injection moldings. part 2: experimental results. *Polym. Comp.* **13**: 332–341, 1992.

[8] S. T. Chung, T. H. Kwon. Numerical simulation of fiber orientation in injection molding of short-fiber reinforced thermoplastics. *Polym. Eng. Sci.* **35**(7): 604–618, 1995.

[9] S. M. Dinh, R. C. Armstrong. A rheological equation of state for semiconcentrated fiber suspensions. *J. Rheol.* **28**(3): 207–227, 1984.

[10] M. Doi, S. F. Edwards. *The Theory of Polymer Dynamics*. Oxford University Press, Oxford et al., 1988.

[11] F. Dupret, A. Couniot, O. Mal, L. Vanderschuren, O. Verhoyen. Modelling and simulation of injection molding. In: D. A. Siginer, D. D. Kee, R. P. Chhabra, eds. *Advances in the Flow and Rheology of Non-Newtonian Fluids*, pages 939–1010. Elsevier, Amsterdam et al., 1999.

[12] F. Dupret, V. Verleye. Modelling of the flow of fiber suspensions in narrow gaps. In: D. A. Siginer, D. D. Kee, R. P. Chhabra, eds. *Advances in the Flow and Rheology of Non-Newtonian Fluids*, pages 1347–1398. Elsevier, Amsterdam et al., 1999.

[13] S. Glaser, K. v. Diest. Berechnungsverfahren für GFK-Bauteile. *Kunststoffe*. **88**(4): 537–542, 1988.

[14] R. P. Hegler. Faserorientierung beim Verarbeiten kurzfaserverstärkter Thermoplaste. *Kunststoffe*. **74**: 271–277, 1984.

[15] R. R. Huilgol, N. Phan-Thien. *Fluid Mechanics of Viscoelasticity*. Elsevier, Amsterdam et al., 1997.

[16] G. B. Jeffery. The motion of ellipsoidal particles immersed in a viscous fluid. *Proc. R. Soc. London*, **A 102**: 161–179, 1922.

[17] W. Michaeli. *Plastics Processing*. Hanser, Munich et al., 1995.

[18] C. J. S. Petrie. The rheology of fibre suspensions. *J. Non-Newtonian Fluid Mech.* **87**: 369–402, 1999.

[19] M. Saito, S. Kukula, Y. Kataoka, T. Miyata. Practical use of statistically modified laminate model for injection moldings. *Material Science and Engineering*. **A285**: 280–287, 2000.

[20] E. Schmachtenberg, N. M. Yazici, O. Schröder. Untersuchung des Langzeitverhaltens von Pumpenbauteilen aus Kunststoff. Abschlußbericht, AIF Forschungsvorhaben, Auftraggeber: WILO GmbH Dortmund, Universität Essen, Institut für Kunststofftechnik und Kunststoffmaschinen, 2000.

[21] C. L. Tucker, S. G. Advani. Processing of short-fiber systems. In: S. G. Advani, eds. *Flow and Rheology in Polymer Composites Manufacturing*, pages 147 – 202. Elsevier, Amsterdam et al., 1994.

[22] B. R. Whiteside, P. D. Coates, P. J. Hine, R. A. Duckett. Glass fibre orientation within injection moulded automotive pedal. simulation and experimental studies. *Plastics, Rubber and Composites*. **29**(1): 38–45, 2000.

[23] M. C. Yeng, C. P. Fung, T. C. Li. The study on the tribological properties of fiber-reinforced pbt composites for various injection molding process parameters. *Wear*. **252**: 934–945, 2002.